

Direct electrochemistry and electrocatalysis of horseradish peroxidase in MnO_2 nanosheet film

XIAO Han, WU JinLing, CHEN Xu & YANG WenSheng[†]

State Key Laboratory of Chemical Resource Engineering, Beijing University of Chemical Technology, Beijing 100029, China

A novel material MnO_2 nanosheet has been used as the support matrix for the immobilization of horseradish peroxidase (HRP). HRP entrapped in MnO_2 nanosheet film exhibits facile direct electron transfer with the electron transfer rate constant of 6.86 s^{-1} . The HRP/ MnO_2 nanosheet film gives a reversible redox couple with the apparent formal peak potential (E°) of -0.315 V (vs. Ag/AgCl) in pH 6.5 phosphate buffer solution (PBS). The formal potential E° of HRP shifts linearly with pH with a slope of $-53.75 \text{ mV} \cdot \text{pH}^{-1}$, denoting that an electron transfer accompanies single-proton transportation. The immobilized HRP shows an electrocatalytic activity to the reduction of H_2O_2 . The response time of the biosensor for H_2O_2 is less than 3 s, and the detection limit is $0.21 \mu\text{mol} \cdot \text{L}^{-1}$ based on signal/noise = 3.

horseradish peroxidase (HRP), MnO_2 nanosheet, direct electrochemistry, H_2O_2

There has been an increasing interest in studying direct electron transfer of redox proteins^[1–4]. The direct electron transfer of redox proteins can serve as a model for the study of metabolic processes in the biological systems and build up a foundation for fabricating a new generation (third generation) of biosensors, catalytic bioreactors, and bio-chips. Due to its commercial availability, horseradish peroxidase (HRP) has long been a representative peroxidase. Each HRP molecule contains a prosthetic heme group as its catalytic site and electro-active center. Electrochemical biosensors based on HRP play important roles in the determinations of H_2O_2 , glucose, hydroxybenzene, and amine. However, it is usually difficult for HRP to realize direct electron transfer on a conventional electrode because of the unfavorable orientation of the protein on electrode surface and the distance between its heme redox center and electrode surface^[5]. It is important to find proper electrode materials and immobilization methods to facilitate the electron transfer.

Nanomaterials provide a new way for the study on bio-electrochemistry because of their remarkable physical and chemical characteristics. Xu et al.^[4] reported that

the direct electron transfer of HRP immobilized in gold nanoparticle film was greatly enhanced. Liu et al.^[6] found that myoglobin (Mb) exhibited facile direct electrochemistry and higher catalytic reactivity in titanate nanotube film than that in nanocrystalline TiO_2 film. It is believed that the introduction of novel nanomaterial with special morphology is a promising approach to greatly enhance electron transfer of Mb. Lvov et al.^[7] fabricated multilayers with MnO_2 nanoparticles, Mb and PDDA. In the multilayers, Mb displayed direct electrochemical behavior and showed catalytic reactivity towards O_2 . MnO_2 nanoparticles have already been used in ascorbic acid^[8] and lactate^[9] biosensors. Strikingly different from nanoparticles, the delaminated colloidal nanosheets have a morphological property of a thickness of molecular dimensions with lateral dimensions of submicrometers to micrometers, so they have received growing attention owing to their extremely high anisotropy, polyelectrolytic nature, etc. Many functional nanosheet materials

Received May 24, 2007; accepted August 3, 2007
doi: 10.1007/s11434-007-0490-8

[†]Corresponding author (email: yangws@mail.buct.edu.cn)

Supported by the National Natural Science Foundation of China (Grant No. 20301002) and the National 863 Program of China (Grant No. 2006AA03Z343)

have been prepared and applied in photochemistry, electrochromic device, and so on^[10]. However, the application of functional nanosheet films in facilitating electron transfer of redox proteins has not been reported so far. In this paper, we have fabricated a novel HRP/MnO₂ nanosheet film. Experimental results reveal that the immobilized HRP in MnO₂ nanosheet film displays direct electrochemical behavior, and shows high catalytic reactivity towards H₂O₂.

1 Experiment

1.1 Chemicals

HRP was obtained from Lizhu Dongfeng Technology Ltd (Shanghai, China). Poly(vinyl butyral) (PVB) was purchased from Sigma. All other chemicals were of analytical grade and used without further purification. Phosphate buffer solutions (PBS) ($0.1 \text{ mol} \cdot \text{L}^{-1}$) of various pH values were prepared by mixing the stock solutions of Na₂HPO₄ and NaH₂PO₄. All aqueous solutions were prepared in doubly distilled water.

Layered manganese oxide was synthesized and then delaminated according to the literature^[11]. Layered manganese oxide was soaked in tetraalkylammonium hydroxide solutions for 7 d. After an appropriate centrifugation procedure (5000 rpm), a brown, well-dispersive colloidal suspension of MnO₂ nanosheets was obtained.

1.2 Preparation of modified electrode

Prior to coating, glassy carbon electrodes (GCE, diameter 3 mm) were polished with 1.0-, 0.3-, 0.05-μm γ-alumina powder, respectively, sonicated in doubly distilled water successively, and then dried with nitrogen. 10 μL of the mixture containing 5.0 g·L⁻¹ HRP and 0.75 g·L⁻¹ MnO₂ nanosheets was cast onto the surface of GCE. The HRP/MnO₂ nanosheet films were dried in air at 4°C in a refrigerator. Then the modified electrodes were dipped into PVB ethanol solution (2% w/w) for 1 min to enhance the adhesive ability and the stability of the films. The modified electrodes were stored in air at 4°C in a refrigerator when not in use.

1.3 Instrumentations

X-ray diffraction (XRD) analysis was carried out using a Shimadzu XRD-6000 diffractometer. Deposit obtained by centrifugation (10000 r/min) of MnO₂ nanosheet colloid was prepared for XRD analysis^[11].

Electrochemical measurements were performed using a CHI660B electrochemistry workstation (Shanghai ChenHua Instrument Co., China). A three-electrode system was used. The reference electrode was an Ag/AgCl (3 mol·L⁻¹ KCl) electrode, the counter electrode was a platinum wire electrode, and the working electrode was a modified GCE. All test solutions were in thoroughly anaerobic conditions by bubbling with high-purity nitrogen through the solutions for at least 30 min, and a nitrogen atmosphere was kept over the solutions during measurements. All measurements were performed at room temperature (approximately 20°C).

2 Results and discussion

2.1 XRD analysis

Figure 1 shows XRD patterns of MnO₂ nanosheets and HRP/MnO₂ nanosheets. The stacked sheets are exfoliated, and each sheet is in irregular orientation in the slurry, so there is no peak in Figure 1a. After air-drying, the layered structure with basal spacing of 0.96 nm reappears as shown in Figure 1b. We can see in Figure 1c that MnO₂ nanosheets remain irregular orientation when the mixture of MnO₂ nanosheets and HRP is dried at 4°C. Below pH 7, HRP (isoelectric point: 8.9) has a net positive charge. It is reasonable that there are electrostatic attractions between the positively charged proteins (size of 6.0 nm×3.5 nm×3.0 nm) and the anionic MnO₂ nanosheets. Thus, restacking does not occur and MnO₂ nanosheets remain the amorphous manner. One molecular layer of water, between the manganese oxide sheets, favors the accommodation of HRP and retention of its activity^[11]. The ideal representation of the structure is shown in Figure 2.

2.2 Direct electrochemistry of HRP

The electrochemical behavior of MnO₂ nanosheets/GCE, HRP/GCE and HRP/MnO₂ nanosheets/GCE was studied by cyclic voltammetry (CV) in a pH 6.5 PBS. As shown in Figure 3a and b, there are no redox peaks for MnO₂ nanosheets/GCE and HRP/GCE within the potential window. A pair of well-defined, quasi-reversible CV peaks located at -0.29 and -0.34 V (vs. Ag/AgCl) are observed on the HRP/MnO₂ nanosheets/GCE (Figure 3c), which is the characteristic of the HRP heme Fe (III)/Fe (II) redox couple. This indicates that the direct electron transfer of HRP can be achieved through the incorporation into MnO₂ nanosheet film. The formal

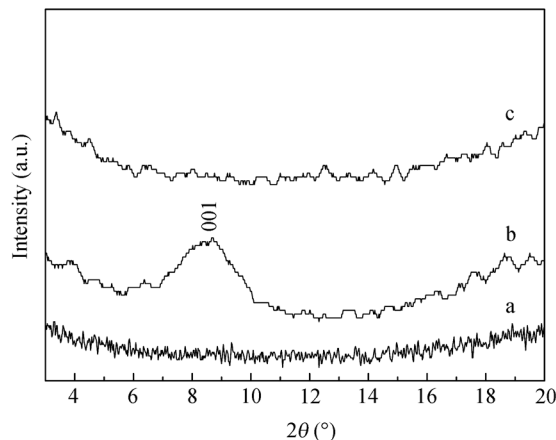


Figure 1 XRD patterns of (a) wet-state MnO_2 nanosheets, (b) MnO_2 nanosheets dried in air, and (c) HRP/ MnO_2 nanosheets.

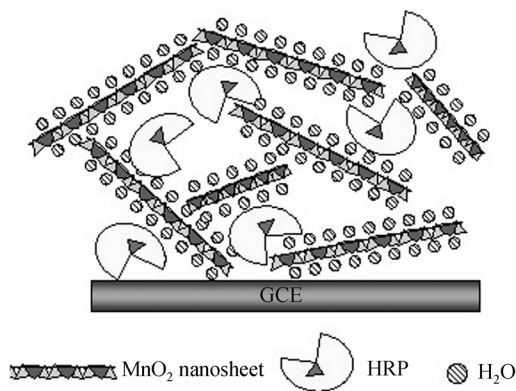


Figure 2 Ideal representation for the structure of the mixture of MnO_2 nanosheets and HRP.

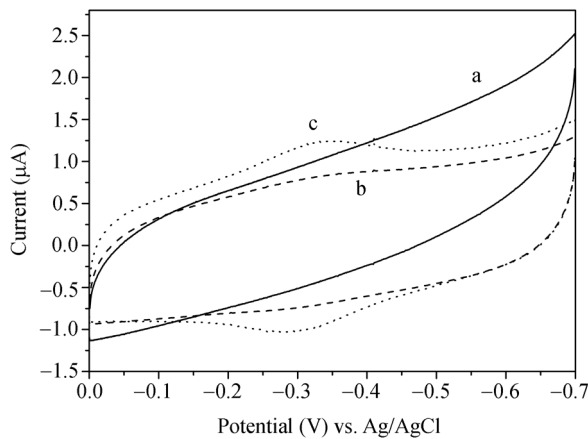


Figure 3 Cyclic voltammograms of (a) MnO_2 nanosheets/GCE, (b) HRP/GCE, and (c) HRP/ MnO_2 nanosheets/GCE in a $0.1 \text{ mol} \cdot \text{L}^{-1}$ PBS (pH 6.5). Scan rate: $100 \text{ mV} \cdot \text{s}^{-1}$.

potential (E^0') is calculated to be -0.315 V vs. Ag/AgCl.

Both the cathodic peak current (i_{pc}) and the anodic peak current (i_{pa}) increase linearly with the increasing

scan rate (Figure 4) and the ratio of i_{pc} to i_{pa} is around 1, indicating a characteristic of a thin-layer electrochemical process. An increase of scan rate leads to a positive shift in potential for anodic peak and a negative shift for cathodic peak, but the values of peak-to-peak separation (ΔE) remain the same, less than 200 mV. Rate constant (k_s) for electron transfer between electrodes and HRP estimated by the method of Laviron^[12] is 6.86 s^{-1} . The k_s value for HRP in carbon nanotube film^[13] is $(2.07 \pm 0.56) \text{ s}^{-1}$, indicating that MnO_2 nanosheet film is an efficient mediator to shuttle electron transfer between the bioactive center of HRP and the surface of GCE.

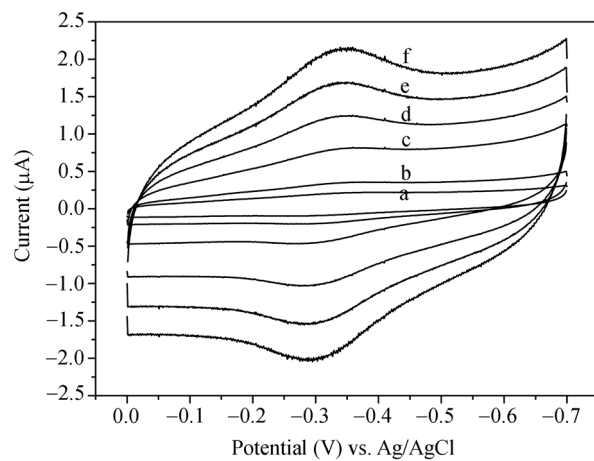


Figure 4 Cyclic voltammograms of HRP/ MnO_2 nanosheets/GCE at 10, 20, 50, 100, 150 and $200 \text{ mV} \cdot \text{s}^{-1}$ (from curve a to curve f) in a $0.1 \text{ mol} \cdot \text{L}^{-1}$ PBS (pH 6.5).

2.3 Influence of pH on direct electrochemistry of HRP

The direct electrochemistry of HRP/ MnO_2 nanosheet film shows a strong dependence on the pH of external solutions. With an increase of solution pH from 4.0 to 8.0, the negative shift of the formal potential E^0' of HRP is observed. In addition, all changes in voltammetric peak potentials and currents with pH are reversible. That is, the same CV is reproduced after immersion in a solution with a different pH and then returns to its original solution. The plot of the formal potential E^0' versus pH (from 4.0 to 8.0) produces a line with a slope of $-53.75 \text{ mV} \cdot \text{pH}^{-1}$, reasonably close to the theoretical value^[14] of $-58 \text{ mV} \cdot \text{pH}^{-1}$ at 20°C for a reversible electrode process coupled by proton transportation with equal number of protons and electrons. This indicates that HRP/ MnO_2 nanosheets/GCE undergoes a single electron, and single proton electrode reaction process.

2.4 Electrocatalytic property of HRP/MnO₂ nanosheets/GCE

HRP/MnO₂ nanosheets/GCE shows a good electrocatalytic property for the reduction of H₂O₂. When a certain volume of H₂O₂ is injected into a pH 6.5 PBS, the cathodic current increases significantly and the anodic current decreases (Figure 5).

To do a control experiment, Figure 6 shows the cyclic voltammograms of MnO₂ nanosheets/GCE in a 0.1 mol·L⁻¹ PBS without and with H₂O₂. The reduction peak of H₂O₂ is at -0.75 V vs. Ag/AgCl, while the reduction peak of H₂O₂ on HRP/MnO₂ nanosheets/GCE is at -0.25 V vs. Ag/AgCl as shown in Figure 5. Thus, the reduction of H₂O₂ on HRP/MnO₂ nanosheets/GCE occurs on the effect of HRP.

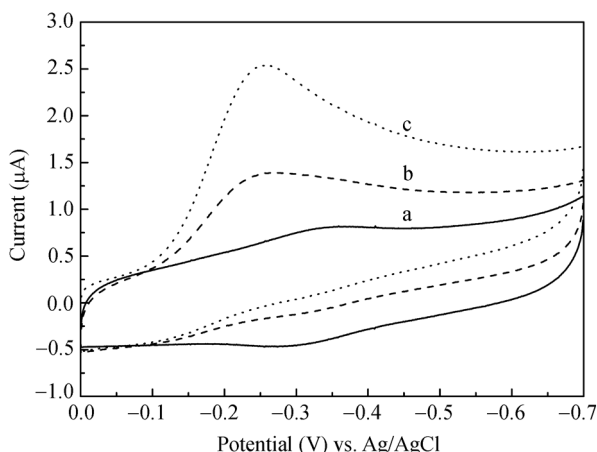


Figure 5 Cyclic voltammograms of HRP/MnO₂ nanosheets/GCE in a 0.1 mol·L⁻¹ PBS (pH 6.5) with (a) 0 mmol·L⁻¹, (b) 0.02 mmol·L⁻¹ and (c) 0.05 mmol·L⁻¹ H₂O₂. Scan rate: 100 mV·s⁻¹.

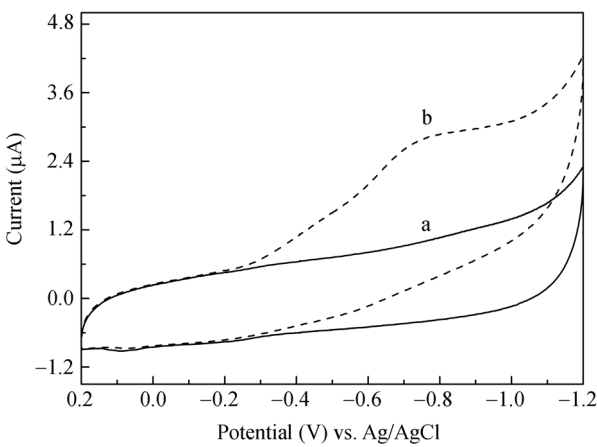


Figure 6 Cyclic voltammograms of MnO₂ nanosheets/GCE in a 0.1 mol·L⁻¹ PBS (pH 6.5) with (a) 0 mmol·L⁻¹ and (b) 0.135 mmol·L⁻¹ H₂O₂. Scan rate: 100 mV·s⁻¹.

In addition, as shown in Figure 5, upon addition of H₂O₂ to PBS, the reduction peak of HRP shifts slightly to negative, which has also been observed in the literature^[15,16]. The possible reasons will need further study.

For MnO₂ nanosheets/GCE (Figure 7a) and HRP/MnO₂ nanosheets/GCE (Figure 7b), at a constant potential of -0.25 V vs. Ag/AgCl, the currents were monitored while aliquots of H₂O₂ were injected into the pH 6.5 PBS. In contrast to HRP/MnO₂ nanosheets/GCE, MnO₂ nanosheets/GCE shows no obvious amperometric behavior with injection of H₂O₂. HRP/MnO₂ nanosheets/GCE exhibits a fast amperometric response to H₂O₂ reduction and reaches steady-state current within 3 s. The linear range for H₂O₂ determination is 1–430 μmol·L⁻¹ with a detection limit of 0.21 μmol·L⁻¹. When the concentration of H₂O₂ is higher than 540 μmol·L⁻¹, a platform is observed, showing the characteristic of the Michaelis-Menten kinetic mechanism. The Michaelis-Menten constant obtained from the Lineweaver-Burk equation^[17] is 0.127 mmol·L⁻¹. The small Michaelis-Menten constant value indicates that HRP entrapped in MnO₂ nanosheet film shows a high peroxidase-like activity.

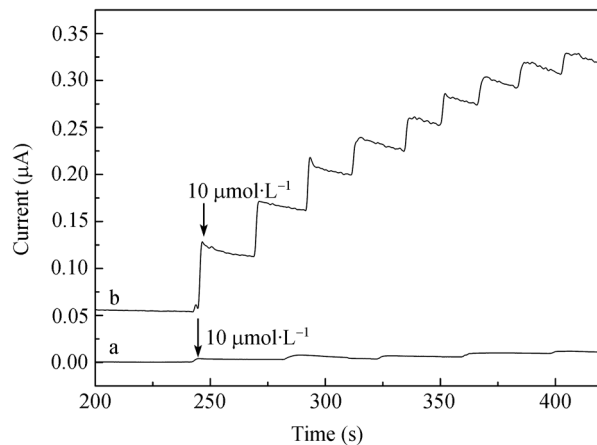


Figure 7 Amperometric responses to H₂O₂ of (a) MnO₂ nanosheets/GCE and (b) HRP/MnO₂ nanosheets/GCE at -0.25 V vs. Ag/AgCl in a 0.1 mol·L⁻¹ PBS (pH 6.5).

In addition, the inhibitory effect of sulfides to HRP was investigated using the method reported by the literature^[18]. As shown in Figure 8, when a certain volume of Na₂S is injected into a pH 6.5 PBS containing 0.5 mmol·L⁻¹ H₂O₂, the cathodic current decreases significantly. The cathodic current decreases with the decreasing concentration of Na₂S, indicating the inhibition effect of Na₂S to HRP. Thus, the determination of Na₂S

can be realized according to the inhibition degree of sulfides to HRP. From current-time plot, the linear range for Na_2S determination is $44\text{--}134 \mu\text{mol}\cdot\text{L}^{-1}$.

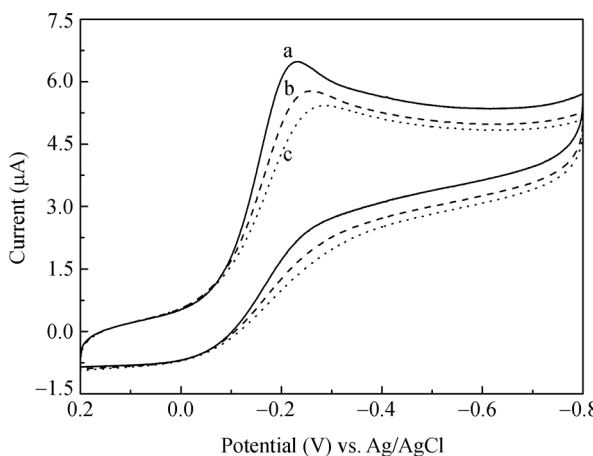


Figure 8 Cyclic Voltammograms of HRP/ MnO_2 nanosheets/GCE in a $0.1 \text{ mol}\cdot\text{L}^{-1}$ PBS (pH 6.5) containing $0.5 \text{ mmol}\cdot\text{L}^{-1}$ H_2O_2 with (a) $0 \mu\text{mol}\cdot\text{L}^{-1}$, (b) $15 \mu\text{mol}\cdot\text{L}^{-1}$ and (c) $30 \mu\text{mol}\cdot\text{L}^{-1}$ Na_2S . Scan rate: $100 \text{ mV}\cdot\text{s}^{-1}$.

2.5 Stability and reproducibility of the modified electrode

When HRP/ MnO_2 nanosheets/GCE has been stored at 4°C in air for two weeks, the modified electrode retains

90% of its initial current response to electrocatalytic reduction of H_2O_2 . The reproducibility of the sensor was examined in five solutions containing $0.01 \text{ mmol}\cdot\text{L}^{-1}$ H_2O_2 with the same modified electrode, and the relative standard deviation is 1.8%. Six electrodes, made independently with the same method, show an acceptable reproducibility with a relative standard deviation of 8.1% for the current response determined at $0.01 \text{ mmol}\cdot\text{L}^{-1}$ H_2O_2 .

3 Conclusions

In this paper, the direct electrochemistry of HRP immobilized in MnO_2 nanosheet film is reported for the first time. In MnO_2 nanosheet film, HRP realizes its direct electron transfer and the electron transfer rate is 6.86 s^{-1} . It is observed that HRP/ MnO_2 nanosheets/GCE exhibits an electrocatalytic activity for the reduction of H_2O_2 . In addition, HRP/ MnO_2 nanosheets/GCE can be used in the determination of sulfide. The results suggest that MnO_2 nanosheet is an excellent matrix for the immobilization of HRP. It is notable that this work provides a method to study other nanosheets (e.g. titanium oxide nanosheet) as promising support to many biological events involving biomacromolecules.

- 1 Armstrong F A, Hill H A O, Walton N J. Direct electrochemistry of redox proteins. *Acc Chem Res*, 1988, 21: 407–413 [[DOI](#)]
- 2 Zhang H, Lu H Y, Hu N F. Fabrication of electroactive layer-by-layer films of myoglobin with gold nanoparticles of different sizes. *J Phys Chem B*, 2006, 110(5): 2171–2179 [[DOI](#)]
- 3 Wu Y H, Shen Q C, Hua S S. Direct electrochemistry and electrocatalysis of heme-proteins in regenerated silk fibroin film. *Anal Chim Acta*, 2006, 558(1-2): 179–186 [[DOI](#)]
- 4 Xu Q, Mao C, Liu N N, et al. Direct electrochemistry of horseradish peroxidase based on biocompatible carboxymethyl chitosan–gold nanoparticle nanocomposite. *Biosens Bioelectron*, 2006, 22(5): 768–773 [[DOI](#)]
- 5 Wang Q L, Lu G X, Yang B J. Myoglobin/sol-gel film modified electrode: Direct electrochemistry and electrochemical catalysis. *Langmuir*, 2004, 20(4): 1342–1347 [[DOI](#)]
- 6 Liu A, Wei M, Honma I, et al. Direct electrochemistry of myoglobin in titanate nanotubes film. *Anal Chem*, 2005, 77(22): 8068–8074 [[DOI](#)]
- 7 Lvov Y, Munge B, Giraldo O, et al. Films of manganese oxide nanoparticles with polycations or myoglobin from alternate-layer adsorption. *Langmuir*, 2000, 16(23): 8850–8857 [[DOI](#)]
- 8 Luo X L, Xu J J, Zhao W, et al. Ascorbic acid sensor based on ion-sensitive field-effect transistor modified with MnO_2 nanoparticles. *Anal Chim Acta*, 2004, 512(1): 57–61 [[DOI](#)]
- 9 Xu J J, Zhao W, Luo X L, et al. A sensitive biosensor for lactate based on layer-by-layer assembling MnO_2 nanoparticles and lactate oxidase on ion-sensitive field-effect transistors. *Chem Comm*, 2005, 5(6): 792–794
- 10 Omomo Y, Sasaki T, Wang L Z, et al. Redoxable nanosheet crystallites of MnO_2 derived via delamination of a layered manganese oxide. *J Am Chem Soc*, 2003, 125(12): 3568–3575 [[DOI](#)]
- 11 Liu Z H, Ooi K, Kanoh H, et al. Swelling and delamination behaviors of birnessite-type manganese oxide by intercalation of tetraalkylammonium ions. *Langmuir*, 2000, 16(9): 4154–4164 [[DOI](#)]
- 12 Laviron E. General expression of the linear potential sweep voltammogram in the case of diffusionless electrochemical systems. *J Electroanal Chem*, 1979, 101: 19–28
- 13 Cai C X, Chen J. Direct electrochemistry of horseradish peroxidase at a carbon nanotube electrode. *Acta Chim Sinica (in Chinese)*, 2004, 62(3): 335–340
- 14 Meites L. *Polarographic techniques*. 2nd ed. New York: Wiley, 1965. 282
- 15 Chen H J, Wang Y L, Liu Y, et al. Direct electrochemistry and electrocatalysis of horseradish peroxidase immobilized in Nafion-RTIL composite film. *Electrochim Commu*, 2007, 9(3): 469–474 [[DOI](#)]
- 16 Zhao G G, Zhang L, Wei X W. An unmediated H_2O_2 biosensor based on the enzyme-like activity of myoglobin on multi-walled carbon nanotubes. *Anal Biochem*, 2004, 329(1): 160–161 [[DOI](#)]
- 17 Feng J J, Zhao G, Xu J J, et al. Direct electrochemistry and electrocatalysis of heme proteins immobilized on gold nanoparticles stabilized by chitosan. *Anal Biochem*, 2005, 342(2): 280–286 [[DOI](#)]
- 18 Yang Y H, Yang M H, Wang H, et al. An amperometric horseradish peroxidase inhibition biosensor based on a cysteamine self-assembled monolayer for the determination of sulfides. *Sensor Actuat B*, 2004, 102(1): 162–168 [[DOI](#)]